The Journal of Immunology

RESEARCH ARTICLE | MARCH 24 2023

Cytotoxic T Cells Targeting Spike Glycoprotein Are Associated with Hybrid Immunity to SARS-CoV-2

Jolie M. Phan; ... et. al

J Immunol (2023) 210 (9): 1236–1246.
https://doi.org/10.4049/jimmunol.2200815

Related Content

A Highly Specific Assay for the Detection of SARS-CoV-2–Reactive $CD4^+$ and $CD8^+$ T Cells in COVID-19 Patients

J Immunol (February,2021)

Roles of glycosylation and redox states on SARS-CoV-2 spike protein actions

J Immunol (May,2023)

Evaluation of the long-term anti-Spike immune response following a novel coronavirus vaccine (CORVax): electroporation of SARS-CoV-2 Spike plasmid DNA plus IL12 plasmid DNA

J Immunol (May,2022)

Downloaded from http://aai.silverchair.com/jimmunol/article-pdf/210/9/1236/1645127/ji2200815.pdf by guest on 09 April 2024

Cytotoxic T Cells Targeting Spike Glycoprotein Are Associated with Hybrid Immunity to SARS-CoV-2

Jolie M. Phan,* Erik D. Layton,* Krystle K. Q. Yu,* Melissa S. Aguilar,* Inah Golez,† Nicholas M. Franko,* Jennifer K. Logue,* Lauren B. Rodda,‡ Christian A. Howard,‡ Marion Pepper,‡ Michael Gale, Jr.,† Helen Y. Chu,*,[1] and Chetan Seshadri*,[1]

mRNA vaccination of individuals with prior SARS-CoV-2 infection provides superior protection against breakthrough infections with variants of concern compared with vaccination in the absence of prior infection. However, the immune mechanisms by which this hybrid immunity is generated and maintained are unknown. Whereas genetic variation in spike glycoprotein effectively subverts neutralizing Abs, spike-specific T cells are generally maintained against SARS-CoV-2 variants. Thus, we comprehensively profiled human T cell responses against the S1 and S2 domains of spike glycoprotein in a cohort of SARS-CoV-2–naive (n = 13) or –convalescent (n = 17) individuals who received two-dose mRNA vaccine series and were matched by age, sex, and vaccine type. Using flow cytometry, we observed that the overall functional breadth of CD4 T cells and polyfunctional Th_1 responses was similar between the two groups. However, polyfunctional cytotoxic CD4 T cell responses against both S1 and S2 domains trended higher among convalescent subjects. Multimodal single-cell RNA sequencing revealed diverse functional programs in spike-specific CD4 and CD8 T cells in both groups. However, convalescent individuals displayed enhanced cytotoxic and antiviral CD8 T cell responses to both S1 and S2 in the absence of cytokine production. Taken together, our data suggest that cytotoxic CD4 and CD8 T cells targeting spike glycoprotein may partially account for hybrid immunity and protection against breakthrough infections with SARS-CoV-2. ***The Journal of Immunology*****, 2023, 210: 1236–1246.**

Large prospective cohort studies have begun to reveal that mRNA vaccination after prior SARS-CoV-2 infection provides better protection against breakthrough infection when compared with vaccination without prior infection. In a recent study from Qatar, mRNA-1273 and BNTb162b2 were associated with a 65% and 72% reduction in breakthrough infections, respectively, with Delta and Omicron variants (1). The magnitude of the protective effect did not seem to wane appreciably over 3 mo of follow-up. These emerging data suggest a significant clinical benefit is achieved when the immune system is first "primed" with SARS-CoV-2 before being "boosted" with mRNA vaccination to mount a hybrid immune response to SARS-CoV-2 infection. However, the immune mechanisms underlying hybrid immunity, that is, immunity acquired from natural infection followed by mRNA vaccination, are still poorly understood.

Neutralizing Abs targeting spike glycoprotein have emerged as a mechanistic correlate of protective immunity against SARS-CoV-2 (2, 3). However, they are highly vulnerable to escape by genetic variation. Both Delta and Omicron variants of SARS-CoV-2 showed significantly reduced sensitivity to sera from convalescent individuals infected with the original Wuhan strain or after mRNA vaccination (4, 5). By contrast, T cell responses appear to be more robust to genetic variation in spike. One study directly examined CD4 and CD8 T cell responses in convalescent donors, as well as vaccinees, and found no differences in reactivity against ancestral spike when compared with Alpha, Beta, Gamma, and Epsilon variants (6). Another study showed that T cell responses to SARS-CoV-2 spike after Omicron infection are also cross-reactive against Alpha, Beta, and Delta variants (7). A detailed repertoire analysis revealed that CD4 and CD8 T cells induced by vaccination recognize a median

*Department of Medicine, University of Washington School of Medicine, Seattle, WA; †Department of Immunology, Center for Innate Immunity and Immune Disease, Washington National Primate Research Center, University of Washington School of Medicine, Seattle, WA; and ‡Department of Immunology, University of Washington School of Medicine, Seattle, WA

[1]H.Y.C. and C.S. contributed equally to this work.

ORCIDs: 0000-0002-2512-868X (J.M.P.); 0000-0001-6409-290X (E.D.L.); 0000-0001-8738-1579 (K.K.Q.Y.); 0000-0001-8165-6332 (N.M.F.); 0000-0002-7889-8960 (J.K.L.); 0000-0001-7763-8166 (L.B.R.); 0000-0002-6332-7436 (M.G.); 0000-0001-8502-9600 (H.Y.C.); 0000-0003-2783-7540 (C.S.).

Received for publication November 2, 2022. Accepted for publication February 22, 2023.

This work was supported by the National Institutes of Health (R01-AI125189 to C.S.). Single-cell sequencing by the Seattle Genomics service core of the Washington National Primate Research Center was also supported by the National Institutes of Health (AI151698 and OD010425 to M.G.).

J.M.P. led data analysis and integration and assisted with flow cytometry experiments. E.D.L. assisted with flow cytometry experiments. K.K.Q.Y. and M.S.A. performed multimodal single-cell RNA sequencing. I.G. and M.G. facilitated sequencing and upstream data processing. J.K.L., N.M.F., and H.Y.C. enrolled the clinical cohort and facilitated access to PBMC and serum samples for the study. L.B.R., C.A.H., and M.P. performed the ELISA experiments and analyzed the data. J.M.P. and C.S. wrote the manuscript with contributions from all authors.

The flow cytometry data presented in this article have been submitted to the ImmPort (https://www.immport.org) under study accession number SDY2159, and the multimodal single-cell RNA sequencing data presented in this article have been submitted to the Gene Expression Omnibus (https://www.ncbi.nlm.nih.gov/geo/) under accession number GSE223236. The code to complete flow cytometry and multimodal single-cell RNA sequencing data analyses can be found at https://github.com/seshadrilab/HAARVIVAC_ICS and https://github.com/seshadrilab/HAARVIVAC_10X, respectively.

Address correspondence and reprint requests to Dr. Chetan Seshadri, University of Washington School of Medicine, 750 Republican Street, Room F871, Seattle, WA 98109. E-mail address: seshadri@uw.edu

The online version of this article contains supplemental material.

Abbreviations used in this article: ADT, Ab-derived tag; CI, confidence interval; COMPASS, Combinatorial Polyfunctionality Analysis of Ag-Specific T Cell Subsets; FS, functionality score; HTO, hashtag oligonucleotide; ICS, intracellular cytokine staining; IFI, IFN-α–inducible; IFIT, IFN-induced protein with tetratricopeptide repeats; MASC, mixed-effects modeling of associations of single cells; NCAP, nucleocapsid; OR, odds ratio; RBD, receptor-binding domain; scRNA-Seq, single-cell RNA sequencing; T_{EMRA}, T effector memory RA; UMAP, uniform manifold approximation and projection; WNN, weighted nearest neighbors.

Copyright © 2023 by The American Association of Immunologists, Inc. 0022-1767/23/$37.50

Downloaded from http://aai.silverchair.com/jimmunol/article-pdf/210/9/1236/1645127/ji2200815.pdf by guest on 09 April 2024

of 11 and 10 spike epitopes, respectively, and ~80% of these responses are maintained against Omicron. Taken together, these data reveal that vaccine-induced T cell responses are largely robust to variation in spike glycoprotein and may contribute to hybrid immunity.

Evidence in support of this hypothesis is emerging. In a study comparing naive or previously infected individuals after two or three doses of mRNA vaccine, we reported that the magnitude of spike-specific CD4 T cells was not significantly different between the groups after vaccination (8). However, the proportion of IFN-γ– and IL-10–producing activated CD4 T cells was increased in previously infected, but not naive, subjects. We also reported higher titers of receptor-binding domain (RBD)-specific Abs and B cells after two, but not three, doses. Another study focused on characterizing epitope breadth and phenotypes of CD8 T cells among naive or previously infected subjects, as well as those who experienced a breakthrough infection (9). Compared with naive subjects, previously infected subjects showed a shift toward T effector memory cells with re-expression of CD45RA (T effector memory RA [T_{EMRA}]) phenotype. They also showed that the clonotype diversity of spike-specific T cells does not narrow after repeat Ag exposure. Taken together, these data suggest that a combination of differences in both the humoral and the cellular response to spike glycoprotein may underlie hybrid immunity.

To more thoroughly investigate potential immune mechanisms underlying hybrid immunity, we comprehensively profiled the functions of T cells targeting the S1 and S2 domains of spike glycoprotein in a cohort of SARS-CoV-2– naive or –convalescent donors who received two doses of mRNA-1273 or BNTb162b2 using flow cytometry and multimodal single-cell RNA sequencing (scRNA-Seq) after matching by age, sex, and vaccine type. The overall polyfunctionality of CD4 T cell responses was remarkably similar between the two groups after vaccination despite a significant difference in prevaccine functional profiles. However, convalescent subjects demonstrated greater magnitudes of cytotoxic CD4 T cell responses to both S1 and S2. Multimodal scRNA-Seq further revealed subpopulations of CD8 T cells that were enriched among convalescent subjects and notable for the expression of cytolytic and antiviral genes in the absence of cytokine production. Together, our data suggest that cytotoxic CD4 and CD8 T cells targeting both conserved and variable regions of spike glycoprotein may partially account for hybrid immunity and protection against breakthrough infections with SARS-CoV-2 variants of concern.

Materials and Methods

Clinical cohort

Subjects were identified through a laboratory alert system, e-mail and flyer advertising, and positive COVID-19 cases reported by the Seattle Flu Study (10). Outpatients completed their enrollment, data collection questionnaire, and first blood draw at an outpatient clinic visit a median of 203 d after symptom onset (or positive test for asymptomatic individuals). All participants subsequently were asked to return for longitudinal follow-up. After U.S. Food and Drug Administration emergency use approval of BNTb162b and mRNA-1273, subjects were recontacted for phlebotomy after vaccination. Samples were collected before vaccination and then at ~10 d after completion of a primary vaccine series. Sociodemographic and clinical data were collected from chart review and from participants at the time of enrollment, including information on the nature and duration of symptoms, medical comorbidities, and care-seeking behavior (11). Prior infection status was determined using spike RBD IgG ELISA, as previously described (8). Samples were selected after matching for age, sex, and vaccine type (Table I). All convalescent subjects were not hospitalized, and three convalescent subjects overlap with a cohort we have previously described (12). Data were generated and analyzed from SARS-CoV-2–naive ($n = 13$) or –convalescent ($n = 17$) donors before or after receipt of two doses of mRNA vaccine.

Sample processing

All whole blood patient samples were collected in acid citrate dextrose or sodium heparin tubes (one subject) and immediately transferred to the University of Washington. Whole blood was centrifuged at 200 × *g* for 10 min to separate plasma. Plasma was collected, centrifuged at 1200 × *g* to remove debris, aliquoted, and stored at −80°C. HBSS (Thermo Fisher Scientific) or 1× PBS (Thermo Fisher Scientific) was added to the whole blood cellular fraction to replace plasma volume. PBMCs were isolated by density-gradient centrifugation using Histopaque (Sigma-Aldrich). After washing, purified PBMCs were resuspended in 90% heat-inactivated FBS (Sigma-Aldrich) with 10% DMSO (Sigma-Aldrich) cryopreservation media and stored in liquid nitrogen until use. Both plasma and PBMCs were frozen within 6 h of collection time.

Ethics

The studies were approved by the University of Washington Human Subjects Institutional Review Board (STUDY00000959), and all participants, or their legally authorized representatives, completed informed consent.

Intracellular cytokine staining

Cryopreserved PBMCs were thawed in sterile-filtered RPMI 1640 (Thermo Fisher Scientific) with 10% FBS (HyClone) and 0.2% Benzonase (MilliporeSigma) and then centrifuged at 300 × *g* for 10 min at room temperature. Viable cells were counted using the Guava easyCyte (MilliporeSigma) with guavaSoft 2.6 software. Cells were centrifuged at 300 × *g* for 10 min at room temperature and rested overnight at a density of 2×10^6 cells/ml. The next day, viable cells were counted using the Guava easyCyte. Stimulation cocktails were prepared with overlapping peptide pools (15 mer overlapping by 11 aa) targeting the S1 or S2 domains of spike glycoprotein or nucleocapsid (NCAP) of the original SARS-CoV-2 strain from Wuhan, Hubei Province, China (JPT Peptide Technologies). The S1 pool spans the N-terminal amino acid residues (1–643 aa, 158 peptides) of spike glycoprotein, whereas the S2 pool spans the C-terminal amino acid residues (633–1273 aa, 157 peptides). Each peptide pool was reconstituted with 55 μl of pure DMSO (Sigma-Aldrich) and then diluted with PBS for a final concentration of 83 or 100 μg/ml in 17% DMSO/83% PBS or 20% DMSO/80% PBS. Stimulation cocktails also consisted of 1 μg/ml CD28/49d (BD Biosciences, San Jose, CA), 10 μg/ml brefeldin A (Sigma-Aldrich), GolgiStop (BD Biosciences) prepared according to the manufacturer's instructions, and anti-CD107a PE-Cy7 (clone H4A3; BD Biosciences). Cells were plated at a density of 1×10^6 cells/well in a 96-well U-bottom plate and stimulated at 37°C with either 1 μg/ml of each peptide in the pool, 0.25 μg/ml staphylococcal enterotoxin type B (List Biological Laboratories), or 0.2% DMSO (Sigma-Aldrich). After 6 h, stimulations were stopped by adding EDTA at a final concentration of 2 mM, and samples were stored overnight at 4°C.

The next day, cells were washed twice with PBS and then stained with Fixable Aqua viability dye (Invitrogen) for 20 min at room temperature. A preparation of anti-CCR7 BV711 (clone 150503; BD Biosciences) in FACS buffer was centrifuged at 10,000 × *g* for 5 min and then added to the cells for 30 min at 37°C. At the end of the incubation period, PBMCs were washed twice with FACS buffer and then incubated for 10 min at room temperature with 1× FACS Lyse (BD Biosciences). After lysis, the cells were washed with FACS buffer twice and then permeabilized by incubating for 10 min at room temperature with 1× FACS Perm II (BD Biosciences). The cells were again washed twice with FACS buffer and then stained with the following markers for 30 min at 4°C before being washed with FACS buffer: anti-CD3 ECD (clone UCHT1; Beckman Coulter), anti-CD4 allophycocyanin-H7 (clone L200; BD Biosciences), anti-CD8β BB700 (clone 2ST8.5H7; BD Biosciences), anti-CD38 BV605 (clone HB7; BD Biosciences), anti–HLA-DR BUV395 (clone G46-6; BD Biosciences), anti-CD40L/CD154 PE-Cy5 (clone TRAP1; BD Biosciences), anti-CD45RA BUV737 (clone HI100; BD Biosciences), anti–IFN-γ V450 (clone B27; BD Biosciences), anti–TNF-α FITC (clone MAb11; BD Biosciences), anti–IL-2 PE (clone MQ1-17H12; BD Biosciences), anti–IL-4 allophycocyanin (clone MP4-25D2; BD Biosciences), anti-CD19 BV785 (clone SJ25C1; BioLegend), anti-CD14 BV785 (clone M5E2; BioLegend), anti–IL-5 allophycocyanin (clone TRFK5; BioLegend), anti–IL-13 allophycocyanin (clone JES10-5A2; BioLegend), and anti–IL-17a Alexa Fluor 700 (clone BL168; BioLegend). Finally, cells were fixed with 1% paraformaldehyde (Electron Microscopy Solution) and washed with PBS. The cells were then resuspended in PBS supplemented with EDTA at a final concentration of 2 mM and stored at 4°C until acquisition. Cells were acquired on a BD LSRFortessa (BD Biosciences) equipped with a high-throughput sampler and configured with blue (488 nm), green (532 nm), red (628 nm), violet (405 nm), and UV (355 nm) lasers using standardized good clinical laboratory practice procedures to minimize variability of data generated. For all flow cytometry

Downloaded from http://aai.silverchair.com/jimmunol/article-pdf/210/9/1236/1645127/ji2200815.pdf by guest on 09 April 2024

experiments, study groups were evenly distributed in each batch, and operators were not blinded to study group assignments.

Cell sorting

Cryopreserved PBMC from SARS-CoV-2–naive ($n = 4$) and –convalescent ($n = 4$) donors collected ~10 d postvaccination were thawed in sterile-filtered RPMI 1640 (Thermo Fisher Scientific) with 10% FBS (Hyclone) and 0.2% Benzonase (MilliporeSigma) and then centrifuged at 300 × *g* for 10 min at room temperature. Viable cells were counted using the Guava easyCyte. Cells were centrifuged at 300 × *g* for 10 min at room temperature and plated at a density of 2×10^6 cells/well in a 96-well U-bottom plate. Next, cells were blocked with 1 μg/ml anti-CD40 (clone HB14; Miltenyi Biotec) at 37°C. After 30 min, cells were stimulated with either 1 μg/ml of S1 or S2 peptide pool, 0.25 μg/ml staphylococcal enterotoxin type B, or 0.5% DMSO for 16 h at 37°C. The following day, cells were washed twice with PBS and stained with Fixable Aqua viability dye (Invitrogen) for 40 min at room temperature. An Ab mixture was prepared for sorting with the following markers: anti-CD7 FITC (clone CD7-6B7; BioLegend), anti-CD69 BV711 (clone FN50; BioLegend), anti-CD137 allophycocyanin/Fire 750 (clone 4B4-1; BioLegend), and anti-CD40L/CD154 PE-Cy5 (clone TRAP1; BD Biosciences). In addition, eight cocktails were prepared with the following TotalSeq-C Ab-derived tags (ADTs): anti-CD3 (clone UCHT1; BioLegend), anti-CD4 (clone RPA-T4; BioLegend), anti-CD8a (clone RPA-T8; BioLegend), anti-GD (clone B1; BioLegend), anti–TRAV1-2 (clone 3C10; BioLegend), anti-CD62L (clone DREG-56; BioLegend), anti-CCR7 (clone G043H7; BioLegend), anti-CD45RA (clone HI100; BioLegend), anti-CD28 (clone CD28.2; BioLegend), anti-CD127 (clone A019D5; BioLegend), anti-CD95 (clone DX2; BioLegend), anti-CXCR3 (clone G025H7; BioLegend), anti-CXCR5 (clone J252D4; BioLegend), anti-CCR4 (clone L291H4; BioLegend), anti-CCR5 (clone J418F1; BioLegend), anti-CCR6 (clone G034E3; BioLegend), anti-CD25 (clone BC96; BioLegend), anti-CD38 (clone HIT2; BioLegend), anti-CD26 (clone BA5b; BioLegend), anti–HLA-DR (clone L243; BioLegend), anti-CD161 (clone HP-3G10; BioLegend), anti-CD103 (clone Ber-ACT8; BioLegend), anti-CD14 (clone M5E2; BioLegend), anti-CD16 (clone 3G8; BioLegend), anti-CD56 (clone 5.1H11; BioLegend), anti-CD11b (clone ICRF44; BioLegend), anti-CD11c (clone S-HCL-3; BioLegend), anti-CD169 (clone 7-239; BioLegend), anti–PD-L1 (clone 29E.2A3; BioLegend), anti-CD19 (clone HIB19; BioLegend), anti-CD20 (clone 2H7; BioLegend), anti-CD163 (clone GHI/61; BioLegend), anti-CD86 (clone IT2.2; BioLegend), anti–mouse IgG2a isotype control (clone MOPC-173; BioLegend), anti–mouse IgG1 isotype control (clone MOPC-21; BioLegend), and anti–mouse IgG2b isotype control (clone MPC-11; BioLegend). One of the following TotalSeq-C anti-human hashtag oligonucleotides (HTOs) was also included in each of the TotalSeq cocktails for cell hashing: hashtag 1 (clones LNH-94/2M2; BioLegend), hashtag 2 (clones LNH-94/2M2; BioLegend), hashtag 3 (clones LNH-94/2M2; BioLegend), hashtag 4 (clones LNH-94/2M2; BioLegend), hashtag 5 (clones LNH-94/2M2; BioLegend), hashtag 6 (clones LNH-94/2M2; BioLegend), hashtag 7 (clones LNH-94/2M2; BioLegend), and hashtag 8 (clones LNH-94/2M2; BioLegend). Cells were stained with the sorting Ab mixture and the appropriate TotalSeq mixture for 30 min at 4°C. Next, cells stimulated with S1 or S2 peptides were separately pooled together and passed through a 35-μm cell strainer. Activated T cells defined as Live/Dead$^-$, CD7$^+$, CD69$^+$, and CD137$^+$ or CD154$^+$ were sorted using a BD FACSAria III Cell Sorter. CD7, a marker for mature T cells, was used for cell sorting instead of CD3 to avoid Ab-binding competition with the ADT panel (13). In total, ~12,600 S1-activated cells and 44,700 S2-activated cells were sorted for downstream analysis.

Multimodal scRNA-Seq and data processing

scRNA-Seq was performed using the Chromium Next GEM Single Cell V(D)J Kit (10× Genomics) according to the manufacturer's instructions. Two wells of a Chromium Next GEM Chip G were loaded with either the pooled S1- or S2-activated T cells. Because of low cell count, samples were not diluted with water before loading into the chip. The Chromium Next GEM Single Cell V(D)J reagent kits (v1.1; 10× Genomics) were used to prepare mRNA, TCR, and surface protein libraries. cDNA amplification and target enrichment were quantified using a Qubit 3 Fluorometer (Invitrogen) and assessed for quality using a 4200 TapeStation System (Agilent). Libraries were constructed and sequenced to a depth of ~11,900 reads per cell using the NextSeq 500 system (Illumina). The Cell Ranger multi pipeline (v5.0.1; 10× Genomics) was used to conduct the alignment and feature expression quantification of the single-cell sequencing data. mRNA and V(D)J reads were aligned to the GRCh38 human reference genome. HTO and ADT reads were aligned to a feature reference containing the appropriate barcode sequences.

Quality control and analysis of the single-cell mRNA and surface protein expression data were performed using the R package Seurat (v4.1.0) (14). Data from the S1- and S2-stimulated samples were processed and analyzed separately using the same procedure. First, HTO data were normalized using the centered log-ratio transformation. Samples were demultiplexed based on HTO enrichment using the *MULTIseqDemux* function, which demultiplexes samples based on the classification method from MULTI-seq (15). This function removes doublets, which represent cell barcodes that cannot be assigned to a single HTO, and negative/ambiguous cell barcodes, which do not clearly express a single HTO above background. Cell barcodes classified as singlets by HTO enrichment were kept and then filtered by gene expression data using the following parameters: (1) >200 unique genes/cell, and (2) <5% mitochondrial counts. Within each cell barcode, the mRNA count data were log normalized, and the ADT count data were centered log-ratio normalized. The normalized ADT expression levels were background corrected based on the 99th percentile expression level of their respective mouse IgG isotype controls, and all negative values were zeroed. A Euclidean distance matrix was constructed from all of the background-corrected ADT data without feature selection and used for uniform manifold approximation and projection (UMAP) visualization and clustering.

From the filtered V(D)J output given by the Cell Ranger multi pipeline, cell barcodes with less than four productive TCR chains or a single productive TCR-β-chain were retained. If a given cell barcode was associated with two TCR-α- or TCR-β-chains, the chain with the greater number of unique molecular identifiers was retained. The R package scRepertoire (v1.4.0) was used to assess clonotype expansion and dynamics (16). Plots were generated using the ggplot2 (v3.3.5) package (17).

Data analysis

Flow cytometry. Data were compensated and gated using FlowJo version 9.9.6 (FlowJo, TreeStar). The intracellular cytokine staining (ICS) flow cytometry data were processed using the OpenCyto framework (v2.6.0) in the R programming environment (18). Combinatorial Polyfunctionality Analysis of Ag-Specific T Cell Subsets (COMPASS; v1.32.0) was used to achieve a comprehensive and unbiased analysis of the functional profiles of Ag-specific T cells (19). COMPASS uses a Bayesian hierarchical framework to model all observed cell subsets and to select those most likely to have Ag-specific responses. COMPASS naturally accounts for high background, such that a cell subset with high background will have lower response probabilities compared with a similar subset with low background. Notably, COMPASS reports only the probability of detecting a particular T cell functional profile rather than the absolute magnitude, which was calculated separately. For a given subject, COMPASS was also used to compute a functionality score (FS) that summarizes the entire functionality profile into a single continuous variable that can be used for standard statistical modeling (e.g., regression). COMPASS was performed on data from each of the Ag stimulations for CD4 T cells. Poor-quality samples were identified within COMPASS by low CD4 or CD8 counts (<3000 cells) and were excluded from downstream analysis. Magnitudes of T cell responses were calculated independent of COMPASS as the proportion of gated events in the stimulated condition. The R package ComplexHeatmap (v2.10.0) was used to visualize COMPASS posterior probabilities of response (20). UMAP visualization was performed on all CD4$^+$ events that were preselected from COMPASS-identified Boolean subsets using the uwot (v0.1.11) package in R with the following parameters: spread = 9, min_dist = 0.02 (21). Fluorescence intensities of each marker were scaled within each batch to achieve a mean of 0 and SD of 1 before UMAP. The following markers were used in the UMAP analysis: CD3, CD4, TNF-α, CD107a, CD40L/CD154, IL-2, IL-17a, IL-4/5/13, IFN-γ, CD45RA, CCR7, CD38, and HLA-DR.

scRNA-Seq. The weighted nearest neighbors (WNN) workflow implemented in Seurat was used to achieve an integrated analysis of gene and surface protein expression data (14). The top 2000 genes with the highest cell-to-cell variance were identified using the *FindVariableFeatures* function with the variance-stabilizing transformation method. The variable genes and all surface protein markers were then scaled and used for dimensional reduction with principal-component analysis. Using the elbow method, the top 8 dimensions of the gene expression data and top 10 dimensions of the surface protein data were selected to construct a WNN graph. The resulting WNN graph was used for integrated UMAP visualization and clustering (resolution = 1). Cell-type clusters were manually annotated based on gene and surface protein expression data. Wilcoxon rank-sum tests were performed on each cluster versus all other cells using the *FindAllMarkers* function with default settings to identify positive differentially expressed genes defining a given cluster. For cluster annotation, genes with a $\log_2$ fold change of at least 1.5 and an adjusted p value <0.05 were considered significantly differentially expressed. In addition, clusters were manually assigned to T cell subsets based on surface

Downloaded from http://aai.silverchair.com/jimmunol/article-pdf/210/9/1236/1645127/ji2200815.pdf by guest on 09 April 2024

protein expression. To assess the associations of infection status with each S1 or S2 WNN-derived cluster, we employed mixed-effects modeling of associations of single cells (MASC) (22). Generalized linear mixed-effects models were estimated using the lme4 package in R (v1.1-29) (23). In the full model, donor was specified as a random effect, and total mRNA count per cell, total ADT count per cell, percent mitochondrial genes per cell, age, and sex were specified as fixed effects. ANOVA was applied to compare the null and full models, and Wald confidence intervals (CIs) and p values were computed. The effect sizes of the associations were estimated by calculating the odds ratio (OR) for each cluster.

Data and code availability

The flow cytometry data supporting this publication are available from ImmPort (https://www.immport.org) under study accession number SDY2159, and the multimodal scRNA-Seq data are available from GEO (https://www.ncbi.nlm.nih.gov/geo/) under the accession number GSE223236. The code to complete flow cytometry and multimodal scRNA-Seq data analyses can be found online at https://github.com/seshadrilab/HAARVIVAC_ICS and https://github.com/seshadrilab/HAARVIVAC_10X, respectively, along with the individual-level metadata used to generate the values in Table I and full lists of positive differentially expressed genes.

Results

Diversity of CD4 T cell responses to spike glycoprotein among SARS-CoV-2–naive donors after mRNA vaccination

We leveraged an existing clinical infrastructure to study immunity to SARS-CoV-2 by enrolling 17 convalescent subjects who elected to receive mRNA vaccine soon after emergency use approval by the U.S. Food and Drug Administration in December 2020. The median time between infection and the baseline blood draw was 203 d, and subjects received their first dose of vaccine a median of 58 d later (Fig. 1A). In parallel, we enrolled 13 subjects without prior SARS-CoV-2 infection who received their first dose of vaccine a median of 28 d after enrollment and baseline blood collection. In both arms, blood was collected and archived on days 9–10 after second vaccine dose (Fig. 1A). Subjects were matched for age, sex, body mass index, and vaccine type (Table I). Infection status was confirmed using IgG ELISA targeting spike RBD, as previously described (8).

We first sought to assess the functional breadth of CD4 T cell responses to the vaccine using multiparameter flow cytometry (Supplemental Fig. 1). In naive individuals, we observed a significant increase in the proportion of $CD154^+$CD4 T cells expressing IFN-γ in response to S1 and S2, but not NCAP, after vaccination (Fig. 1B, 1C). These data are consistent with published data from early-phase clinical trials of BNT162b and mRNA-1273 (24, 25). To more comprehensively assess the functional diversity of vaccine-induced T cell responses among SARS-CoV-2–naive subjects, we employed COMPASS, which reports the probability of detecting a response above background among all possible functional subsets (19). Results can also be summarized into a "functionality score," which facilitates standard statistical modeling. COMPASS detected responses above background in 17 of 128 possible CD4 functional subsets (Fig. 1D). Eight subsets exhibited three or more functions simultaneously, including the Th_1 (IFN-γ), Th_2 (IL-4/5/13), cytotoxicity (CD107a), and B cell help (CD154) functions. Several spike-specific monofunctional CD4 T cell subsets were observed before vaccination. Prevaccination FSs were also higher in response to S2 stimulation compared with NCAP or S1 (Supplemental Fig. 2A). These results are likely due to pre-existing cross-reactivity of S2-specific T cells with endemic coronaviruses (26–28). In addition, we noted a significant increase in the functional breadth of CD4 T cell responses to S1 and S2, but not NCAP, after mRNA vaccination (Fig. 1E). Because COMPASS reports only the probability of detecting a functional response, we next examined the magnitudes and phenotypes of COMPASS selected subsets. Of the 17 subsets identified after stimulation with S1 or S2 peptide pool, six subsets characterized by combinations of Th_1 and Th_2 cytokines showed statistical evidence of expansion after vaccination (unadjusted $p < 0.05$; Supplemental Fig. 2C, 2D). Highly polyfunctional $CD4^+$ T cells expressed an effector memory phenotype ($CD45RA^-CCR7^-$) and showed expression of in vivo activation markers HLA-DR and CD38 (Fig. 1F). Specifically, we noted an increase in the magnitudes of S1- and S2-specific T cells expressing HLA-DR or an effector memory phenotype after vaccination (Fig. 1G, 1H). Taken together, these data confirm and expand previously published studies by revealing the induction of functionally diverse memory CD4 T cells targeting S1 and S2 in SARS-CoV-2–naive individuals after mRNA vaccination (29).

Preferential induction of cytotoxic CD4 T cell responses to spike glycoprotein in SARS-CoV-2–convalescent donors after mRNA vaccination

We next sought to assess the functional breadth of CD4 T cell responses to mRNA vaccination in convalescent individuals and contrast that with naive individuals. Consistent with published reports, we observed high baseline frequencies of $CD154^+$ CD4 T cells expressing IFN-γ in response to stimulation with NCAP, S1, and S2 (Fig. 2A, 2B) (12, 30). Frequencies of IFN-γ^+ CD4 T cells targeting S1 and S2, but not NCAP, were increased after vaccination (Fig. 2B). Surprisingly, these frequencies were not significantly different between naive and convalescent individuals (Fig. 2C). COMPASS identified 18 of 128 possible CD4 functional subsets that largely mirrored what was observed in naive individuals (Fig. 2D). Prevaccination FSs were lower in response to NCAP stimulation than S1 or S2 (Supplemental Fig. 2B). There was no difference in the median FSs of CD4 T cell responses targeting S1 and S2 after vaccination (Fig. 2E). Increases in the frequencies of several highly polyfunctional profiles contributed to functional breadth observed in convalescent individuals (Supplemental Fig. 3A, 3B). Compared with naive subjects, highly polyfunctional CD4 T cells expressed CD38 rather than HLA-DR but were also skewed toward an effector memory phenotype (Supplemental Fig. 3C–E). Notably, we observed a vaccine-induced increase in the frequency of IFN-γ^+ $CD107a^+$ CD4 T cells in response to both S1 and S2 (Fig. 2F, 2G). The frequency of IFN-$\gamma^+CD107a^+$ CD4 T cells was 3.40- and 2.73-fold greater in convalescent subjects than naive subjects in response to stimulation with S1 and S2, respectively, but this difference was not statistically significant after correcting for multiple-hypothesis testing (Fig. 2H). There was no difference in the overall functional breadth of CD4 T cell responses between naive and convalescent individuals after vaccination (Fig. 2I). Together, these data reveal that convalescent individuals develop a functionally diverse CD4 T cell response to mRNA vaccination with a skew toward cytotoxic phenotypes when compared with naive individuals.

Multimodal scRNA-Seq reveals functional diversity of spike-specific T cells after mRNA vaccination

Having identified broadly similar vaccine-induced CD4 T cell functional profiles between naive and convalescent individuals, we then sought to more accurately compare Ag-specific T cells using multimodal (surface protein, gene expression, and TCR clonotype) single-cell RNA sequencing. PBMCs obtained 9–10 d postvaccination from naive ($n = 4$) or convalescent ($n = 4$) subjects were stimulated with S1 or S2 peptide pools, labeled with a panel of ADTs, and sorted based on expression of T cell (CD7) and activation markers (CD69, CD137, and CD154) (Supplemental Fig. 4A, 4B). Although cells were sorted for activated T cells before performing multimodal scRNA-Seq, non-T cells were identified on the basis of ADT expression. Clusters were annotated by ADT expression as "CD4 T cells," "CD8 T cells," "NK cells," "DCs" (dendritic cells),

Downloaded from http://aai.silverchair.com/jimmunol/article-pdf/210/9/1236/1645127/ji2200815.pdf by guest on 09 April 2024

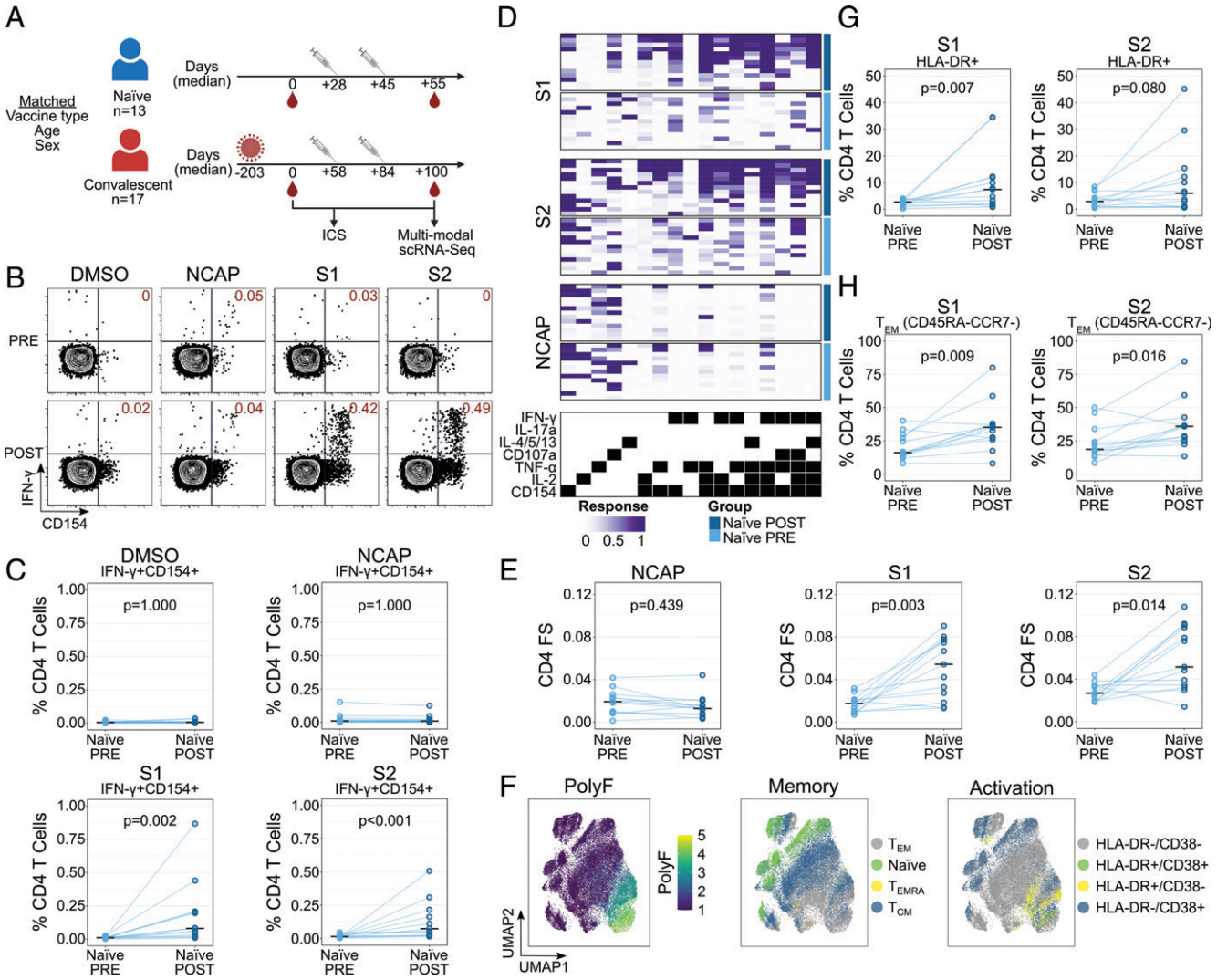

FIGURE 1. Diversity of CD4 T cell responses to spike among SARS-CoV-2–naive donors after mRNA vaccination. (**A**) Study schema. PBMCs from donors who are SARS-CoV-2 naive (blue, $n = 13$) or convalescent (red, $n = 17$) were selected based on matching for vaccine type, age, and sex. Samples were analyzed before and after mRNA vaccination with flow cytometry and ICS. Multimodal scRNA-Seq was used only to profile samples collected after vaccination. Time points are relative to the prevaccination blood draw date. (**B**) Representative staining of CD4 T cells expressing IFN-γ and/or CD154 in a naive donor in response to stimulation with DMSO, NCAP, S1, or S2 peptide pools. (**C**) Frequencies of CD4 T cells coexpressing IFN-γ and CD154 among naive donors before and after vaccination following stimulation with DMSO, NCAP, S1, or S2 peptide pools. A single outlier is not displayed for S2. (**D**) Results from COMPASS analysis of ICS data derived from naive donors are displayed as a probability heatmap. Columns represent the functional CD4 T cell subsets ordered by degree of functionality, and rows represent samples ordered by stimulation and time point. The depth of purple shading corresponds to the probability that a donor exhibits a response above background for a given cell subset. (**E**) CD4 T cell FSs of naive donors after stimulation with NCAP, S1, or S2 peptide pools. (**F**) CD4 T cells expressing any of the functional profiles identified by COMPASS were aggregated across all naive donors before performing dimensionality reduction with UMAP. UMAP visualizations are colored by activation markers (HLA-DR, CD38) and memory markers (naive, $CD45RA^+CCR7^+$; central memory [T_{CM}], $CD45RA^-CCR7^+$; effector memory [T_{EM}], $CD45RA^-CCR7^-$; and T_{EMRA}, $CD45RA^+CCR7^-$). Polyfunctionality (PolyF) was calculated as the number of cytokines gated positive for each cell. (**G** and **H**) Frequencies of S1- and S2-specific $HLA\text{-}DR^+$ (G) and effector memory ($CD45RA^-CCR7^-$) (H) CD4 T cells identified by COMPASS among naive donors. Significance was determined by Wilcoxon signed-rank tests in (C), (E), (G), and (H) and include outliers that are not displayed. All p values were corrected for multiple-hypothesis testing using the Bonferroni method.

or "B cells" (Supplemental Fig. 4E). Only cell barcodes annotated as "CD4 T cells" or "CD8 T cells" were retained for further analysis. After quality-control filtering, a total of 7694 cells were analyzed with an average of 481 cells per donor, which did not differ between the groups (Supplemental Fig. 4C–F). WNN analysis of protein and gene expression data revealed 15 S1-specific T cell clusters, including 10 expressing CD4, 4 expressing CD8, and 1 unassigned (Fig. 3A). Clusters were further defined and annotated based on protein and differential gene expression analysis (Fig. 3B, 3C). CD4 and CD8 T cells expressing the highest levels of CD45RA, CCR7, and CD62L while lacking CD95 also expressed transcription factor *TCF7*, and long noncoding RNA *MALAT1* were designated as naive-like T cells (31, 32). Mucosal-associated invariant T (MAIT) cells were identified via expression of canonical markers CD8, TRAV1-2, CD161, and CD26 (33). Two clusters of CD8 T cells expressed cytotoxic gene signatures (*CCL5*, *NKG7*, *XCL1*, *XCL2*, *GZMB*, and *GNLY*) but were distinguished by surface expression of CD45RA or activation markers (CD38,

Downloaded from http://aai.silverchair.com/jimmunol/article-pdf/210/9/1236/1645127/ji2200815.pdf by guest on 09 April 2024

Table I. Summary of clinical and demographic characteristics of study subjects

	SARS-CoV-2 Naive	SARS-CoV-2 Convalescent
Total, *n*	13	17
Age, median (range), y	42 (25–77)	45 (25–76)
Sex (female:male), *n*	8:5	9:8
Race/Ethnicity		
White, non-Hispanic/Latino	10 (76.9)	13 (76.5)
Black, non-Hispanic/Latino	1 (7.7)	0 (0.0)
Other, non-Hispanic/Latino	2 (15.4)	3 (17.6)
Hispanic/Latino	0 (0.0)	1 (5.9)
BMI, median (range)	29.2 (19.0–42.8)	27.8 (19.5–33.0)
Pre-existing conditions, *n* (%)		
Asthma	2 (15.4)	0 (0.0)
Cancer	0 (0.0)	1 (5.9)
Chronic kidney disease	0 (0.0)	1 (5.9)
COPD/emphysema	1 (7.7)	0 (0.0)
Diabetes	1 (7.7)	0 (0.0)
Hypertension	0 (0.0)	2 (11.8)
Vaccine type, *n* (%)		
Moderna	6 (46.2)	8 (47.1)
Pfizer	7 (53.8)	9 (52.9)
Seronegative at date of prevaccination draw, *n* (%)	13 (100.0)	–
Days between symptom onset and postvaccination draw, median (range)	–	303 (123–398)

Archived blood samples were selected from naive and convalescent donors after matching for age, sex, and vaccine type. Number of donors, age, sex, race/ethnicity, BMI, pre-existing conditions, vaccine type, serostatus, and days between symptom onset and postvaccination blood draw are indicated. Serostatus against SARS-CoV-2 of the naive donors before vaccination was confirmed by spike RBD IgG ELISA.

BMI, body mass index; COPD, chronic obstructive pulmonary disease.

HLA-DR, CD86, CD11b, CD11c). These were designated "T_{EMRA} Cytotoxic CD8" or "Activated Cytotoxic CD8," respectively (34, 35). Similarly, two effector memory CD4 T cell clusters expressed cytotoxic markers but were distinguished by CCR5, CD161, and CD26 protein expression and designated as "Activated Cytotoxic CD4" or "$CCR5^+CD26^+CD161^+$ Cytotoxic CD4." One cluster of effector CD4 T cells also expressed CD38, as well as genes *IL2*, *IFN-γ*, and *FABP5*, consistent with our flow cytometry data (Fig. 1F), and was labeled "Activated Th_1 CD4." Notably, cytotoxic function and cytokine expression were largely mutually exclusive (Fig. 3B). Three clusters of memory CD4 T cells were characterized by varying expression of CCR6 and CCR4, as well as antiviral IFN-induced protein with tetratricopeptide repeats (*IFIT*) genes or CXCR4 (36). Finally, we were able to identify S1-specific regulatory T cells by protein (CD25, PD-L1) and gene expression (*FOXP3*, *LGALS3*), as well as resident memory T cells by CD103 expression (37). These data reveal the diversity of S1-specific CD4 and CD8 T cells, including those that display broad cytotoxic function and antiviral function in the absence of cytokine production.

Preferential induction of cytotoxic CD8 T cell responses to spike glycoprotein in SARS-CoV-2–convalescent donors after mRNA vaccination

Multimodal analysis of S2-specific T cells revealed a similar pattern (Fig. 3B, 3C). Cluster 11 was "Unassigned" and excluded from further analysis based on costaining with the dendritic cell marker CD123 (data not shown). We noted the same three subpopulations of cytotoxic CD8 T cells: mucosal-associated invariant T, activated, and T_{EMRA}. Among CD4 T cells, we noted regulatory T cells and resident memory T cells, as well as both activated Th_1 and cytotoxic clusters. Three additional clusters of memory CD4 T cells could be defined based on CCR4, CCR6, and expression of *IFIT* genes or CXCR4. Clonotype analysis confirmed the naive-like T cell clusters as having the lowest proportion of expanded clones (Fig. 4A). By contrast, the clusters with the highest proportion of expanded clones in response to S1 stimulation were Activated Cytotoxic CD8 (32.11%) and T_{EMRA} Cytotoxic CD8 (17.89%). Similarly, 62.26% of Activated Cytotoxic CD8 and 23.45% of T_{EMRA} Cytotoxic CD8 clones were expanded in response to S2 stimulation (Fig. 4A). We used MASC to determine the quantitative associations between cell clusters and either naive or convalescent subjects (22). After stimulation with S1 peptide pool, two clusters showed modest association with naive subjects: Activated Th_1 CD4 (OR = 0.59; 95% CI: 0.33–1.07) and $CCR5^+CD26^+CD161^+$ Cytotoxic CD4 (OR = 0.62; 95% CI: 0.39–0.98). By contrast, T_{EMRA} Cytotoxic CD8 was strongly associated with convalescent subjects (OR = 2.63; 95% CI: 1.28–5.42). MASC analysis of data obtained after stimulation with S2 peptide pool yielded a similar pattern. Again, Activated Th_1 CD4 was significantly associated with naive subjects (OR = 0.55; 95% CI: 0.35–0.87). In contrast, Activated Cytotoxic CD8 was strongly associated with convalescent subjects (OR = 14.20; 95% CI: 2.34–86.14). Taken together, these results reveal the preferential expansion of cytotoxic CD8 T cells targeted both the S1 and the S2 domains of spike glycoprotein after mRNA vaccination among individuals with prior SARS-CoV-2 infection.

Discussion

In summary, we performed a cross-sectional study comprehensively examining the functional profiles of T cells targeting SARS-CoV-2 spike glycoprotein in vaccinated individuals who were either previously infected with or naive to SARS-CoV-2 after matching for age, sex, and vaccine type. Although we found that cytotoxic CD4 T cell responses appeared to trend higher in convalescent subjects, the overall functional breadth of spike-specific CD4 T cells was similar between the two groups. Multimodal single-cell analysis revealed a diversity of both CD4 and CD8 functional profiles targeting both S1 and S2. Notably, these subsets included cytotoxic and antiviral programs in the absence of cytokines that are typically the focus of immunogenicity studies (24, 38–40). Detection of activated cytotoxic or T_{EMRA} CD8 T cells after vaccination was highly associated with prior SARS-CoV-2 infection. Our data suggest that the enhanced protection afforded by hybrid immunity, defined in this article as infection followed by primary mRNA vaccination, against breakthrough infections may be partially mediated by spike-specific CD4 and CD8 T cells that are programmed to directly lyse target cells infected with SARS-CoV-2.

Downloaded from http://aai.silverchair.com/jimmunol/article-pdf/210/9/1236/1645127/ji2200815.pdf by guest on 09 April 2024

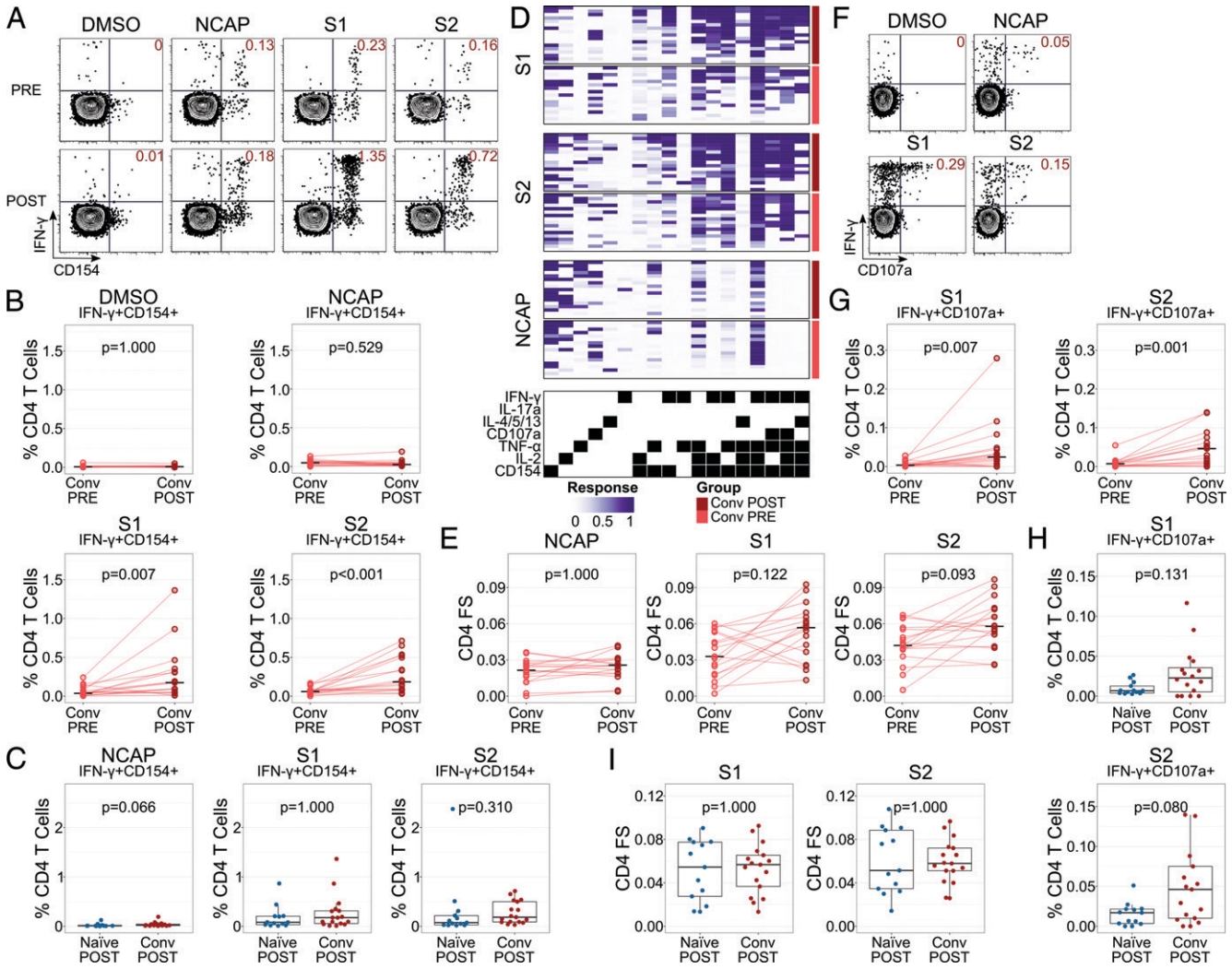

FIGURE 2. Preferential induction of cytotoxic CD4 T cell responses to spike in SARS-CoV-2–convalescent donors after mRNA vaccination. (**A**) Representative staining of CD4 T cells expressing IFN-γ and/or CD154 in a convalescent donor in response to stimulation with DMSO, NCAP, S1, or S2 peptide pools. (**B**) Frequencies of CD4 T cells coexpressing IFN-γ and CD154 among naive donors before and after vaccination following stimulation with DMSO, NCAP, S1, or S2 peptide pools. (**C**) Comparison of frequencies of CD4 T cells coexpressing IFN-γ and CD154 between naive and convalescent donors after vaccination in response to stimulation with NCAP, S1, or S2 peptide pools. (**D**) Results from COMPASS analysis of ICS data derived from convalescent donors are displayed as a probability heatmap. Columns represent the functional CD4 T cell subsets ordered by degree of functionality, and rows represent samples ordered by stimulation and time point. The depth of purple shading corresponds to the probability that a donor exhibits a response above background for a given cell subset. (**E**) CD4 T cell FSs of convalescent donors after stimulation with NCAP, S1, or S2 peptide pools. (**F**) Representative staining of CD4 T cells expressing IFN-γ and/or CD107a in a convalescent donor in response to stimulation with DMSO, NCAP, S1, or S2 peptide pools. (**G**) Frequencies of S1- or S2-specific CD4 T cells coexpressing IFN-γ and CD107a before and after vaccination among convalescent donors. A single outlier is not displayed for S2. (**H**) Comparison of the frequencies of CD4 T cells coexpressing IFN-γ and CD107a between naive and convalescent donors after vaccination in response to stimulation with S1 or S2 peptide pools. A single outlier is not displayed for S1. (**I**) CD4 T cell FSs of vaccinated naive and convalescent donors after stimulation with S1 or S2 peptide pools. Comparisons across time point and infection status in (B), (C), (E), and (G)–(I) were made by Wilcoxon signed-rank and rank-sum tests, respectively, and include outliers that are not displayed. All *p* values were corrected for multiple-hypothesis testing using the Bonferroni method.

BNT162b2 effectively induces CD8 T cells and may account for the protection afforded by prime vaccination before peak induction of neutralizing Abs by boost vaccination (29, 41). Low-dose (25 μg) mRNA-1273 vaccine also induced CD8 T cells in the majority of subjects (42). In rhesus macaques, CD8 T cells provided partial protective immunity against SARS-CoV-2 challenge in the context of suboptimal Ab titers, supporting their definition as mechanistic correlates of protective immunity (2, 43). In most studies, Ag-specific CD8 T cells are quantified by the expression of cytokines, such as IFN-γ, or activation markers, but cytotoxic function is not typically assessed. Our data extend these published studies by revealing that cytotoxic programs expressed by spike-specific CD4 and CD8 T cells may underlie hybrid immunity. In support of our finding, a recent study also reported a shift toward T_{EMRA} CD8 T cells in convalescent compared with naive subjects (9). MASC analysis revealed a 5-fold stronger association with S2 compared with S1 (OR = 14.2 versus 2.63; Fig. 4B). This is consistent with recent studies showing stronger vaccine-induced functional humoral immune responses against S2 rather than S1 after prior infection with SARS-CoV-2 (P. Kaplonek, Y. Deng, J. S.-L. Lee, H. J. Zar, D. Zavadska, M. Johnson, D. A. Lauffenburger, D. Goldblatt, and G. Alter, manuscript posted on medRxiv, DOI: 10.1101/2022.06.28.22276786; R. P. McNamara, J. S. Maron, H. L. Bertera, J. Boucau, V. Roy, A. K. Barczak; The Positives Study Staff; N. Franko, J. Z. Li, J. S. McLellan, M. J. Siedner, et al., manuscript posted on bioRxiv, DOI: 10.1101/2022.06.19.496718).

Downloaded from http://aai.silverchair.com/jimmunol/article-pdf/210/9/1236/1645127/ji2200815.pdf by guest on 09 April 2024

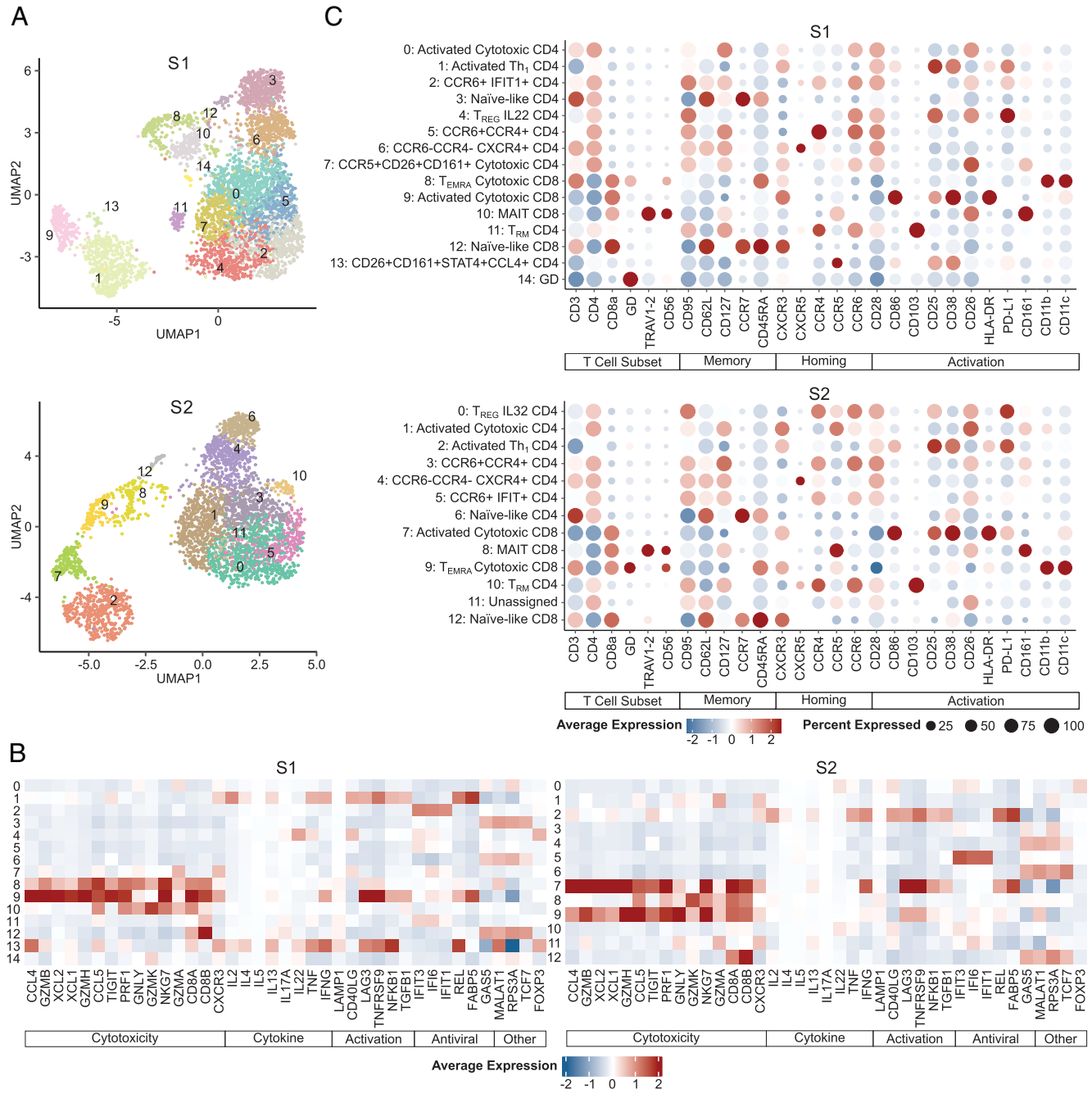

FIGURE 3. Multimodal scRNA-Seq reveals functional diversity of spike-specific T cells after mRNA vaccination. The cumulative data shown are from naive ($n = 4$) and convalescent ($n = 4$) donors after vaccination. (**A**) UMAP visualizations of mRNA and protein expression data integrated by WNN analysis. Cells stimulated by S1 or S2 peptide pools were analyzed separately. S1-specific T cells are colored by 15 multimodal clusters, and S2-specific T cells are colored by 13 multimodal clusters. (**B**) Heatmaps display the average expression of selected genes across S1 or S2 WNN-derived T cell clusters. (**C**) Dot plots display the average expression of selected surface proteins across S1 or S2 WNN-derived T cell clusters. The size of the dots reflects the proportion of cells expressing a particular marker, and the color represents the magnitude of expression. Clusters were annotated based on surface proteins and differentially expressed genes. Expression values were scaled for each marker independently in (B) and (C), with percent mitochondrial genes regressed out in (B).

Another cytokine-independent program we observed was the expression of IFN-α–inducible (*IFI*) and *IFIT* genes by spike-specific CCR6$^+$ CD4 T cells. These protein families have been shown broadly to mediate protective immunity in human viral infection (36). In the context of SARS-CoV-2, expression of *IFIT1*, *IFIT3*, and *IFI6* genes in macrophages obtained from bronchoalveolar lavage was associated with viral clearance and recovery (44). Expression of *IFIT1*, *IFIT3*, and *IFI6* in blood monocytes has also been associated with improved clinical outcomes after COVID-19 (45). Our data extend these results by revealing the association between this protective transcription program and spike-specific CD4 T cells expressing CCR6, which binds CCL20 and has a role in mediating mucosal immune responses (46, 47).

Clinical support for vaccination after natural infection is limited but beginning to emerge. In a landmark study, Abu-Raddad et al. (1) leveraged a national database in Qatar to show that receipt of the two-dose primary series of mRNA-1273 and BNTb162b2 was associated with a 65% and 72% reduction in breakthrough infections,

Downloaded from http://aai.silverchair.com/jimmunol/article-pdf/210/9/1236/1645127/ji2200815.pdf by guest on 09 April 2024

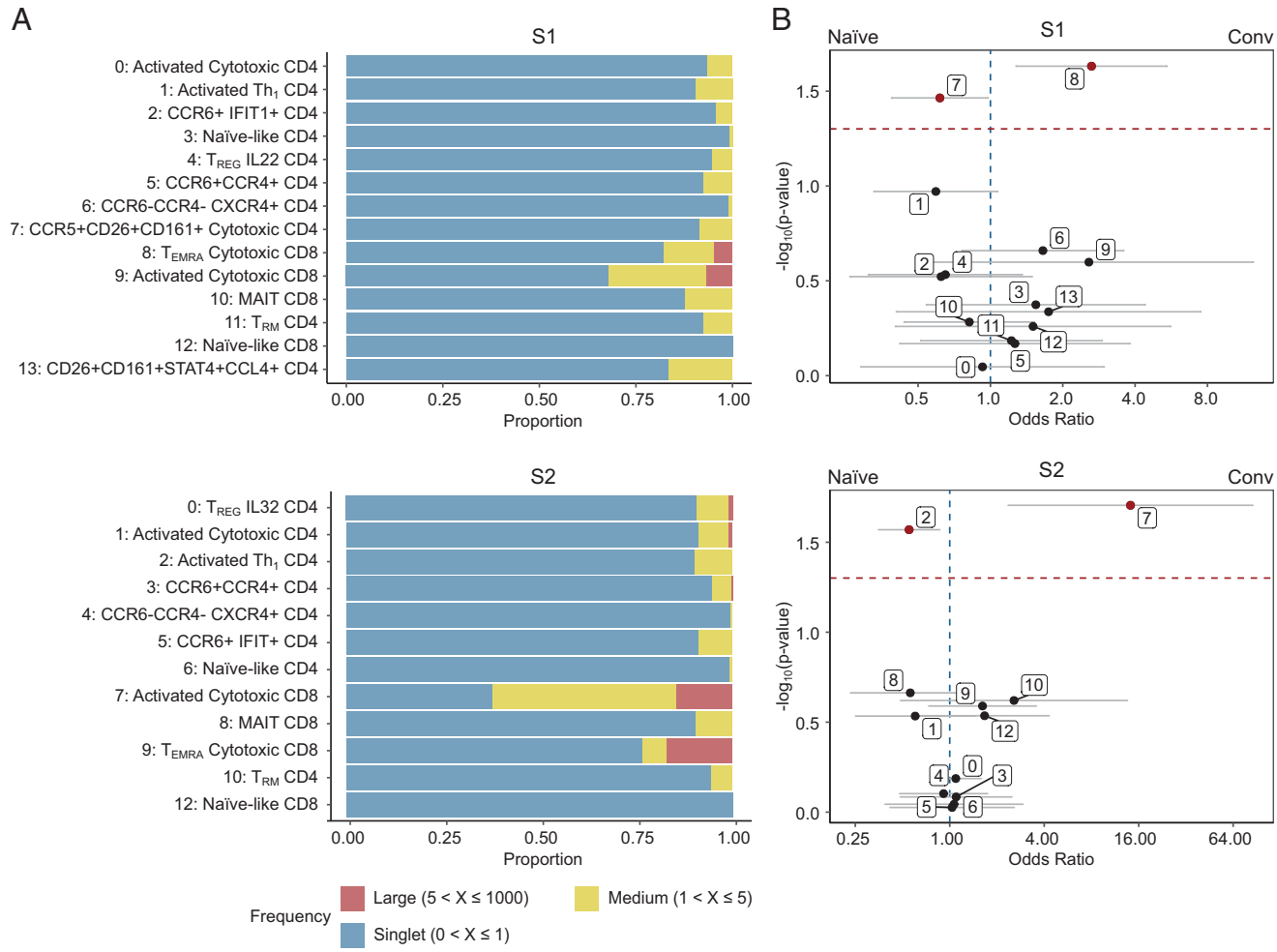

FIGURE 4. Preferential induction of cytotoxic CD8 T cell responses to spike in SARS-CoV-2–convalescent donors after mRNA vaccination. (**A**) TCR clonotypes were defined by the amino acid sequences of the TCR CDR3. Frequencies were binned as singlets ($0 < x \leq 1$), medium ($1 < x \leq 5$), and large ($5 < x \leq 1000$) to determine clonotype expansion. Stacked bar graphs display the frequency distribution of different clonotypes by S1 or S2 WNN-derived clusters. S1 cluster 14 ("GD") and S2 cluster 11 ("Unassigned") are not shown. (**B**) Associations between infection status and S1 or S2 WNN-derived clusters were determined by MASC. Models were adjusted for donor, total RNA count per cell, total ADT count per cell, percent mitochondrial genes per cell, age, and sex. Significance of associations was tested by ANOVA, and all p values are unadjusted. Data are displayed with point estimates of the OR of cells in each WNN-derived cluster being associated with convalescent or naive donors, as well as the 95% CI and the $-\log_{10}(p \text{ value})$ of the association. The red dashed horizontal line corresponds to a nominal p value of 0.05.

respectively, with Delta and Omicron variants. In a follow-up study, they showed that protection against symptomatic SARS-CoV-2 infection from a third (booster) dose alone is comparable with that of hybrid immunity from prior infection and the primary vaccine series (~50%) (48). The greatest protection was observed with prior infection and booster vaccination (~80%) and appeared to be additive. This suggests that vaccination is still beneficial even for those who have been previously infected, and demonstrates the durable immune response from natural infection. Notably, the protection conferred by hybrid immunity does appear to wane over time, but much more slowly than with vaccination alone (1). Our data add to the existing literature by revealing the contribution of cytokine-independent T cell functions in mediating this protection. In our study, a median of 203 d had elapsed between infection and first vaccine dose, possibly accounting for some of the negative or statistically marginal associations we observed. Even though current Centers for Disease Control and Prevention guidelines recommend up to five vaccine doses, including a bivalent booster, clinical evidence in support of more than three vaccine doses is still limited (49). SARS-CoV-2 spike-specific T cell responses have been observed to remain stable despite additional booster doses across different vaccine platforms and regimens (50). Evaluating T cell responses induced by different SARS-CoV-2 vaccine platforms and regimens may provide greater understanding of protective T cell immunity. Adenovirus-based vector vaccines, such as the ChAdOx1 nCoV-19 vaccine, have also been shown to induce lasting T cell immunity against spike glycoprotein despite declining Ab activity over time, although reports suggest that the T cell responses generated by mRNA or heterologous SARS-CoV-2 vaccination are greater in frequency and intensity (50–52).

Our data thus reveal at least two functional programs expressed by SARS-CoV-2 spike-specific T cells that are independent of IFN-γ and other cytokines typically associated with antiviral T cell immunity. Expression of *IFI/IFIT* genes by CD4 T cells was observed in both naive and convalescent individuals after mRNA vaccination. However, expression of cytotoxic CD4 and CD8 functions was enhanced among those who were vaccinated after SARS-CoV-2 infection. Given the small sample size of our multimodal scRNA-Seq data, this study may be statistically underpowered to identify additional expanded T cell subsets that differentiate convalescent from naive individuals after mRNA vaccination. Moreover, although this study focuses on hybrid immunity acquired by infection

Downloaded from http://aai.silverchair.com/jimmunol/article-pdf/210/9/1236/1645127/ji2200815.pdf by guest on 09 April 2024

followed by primary mRNA vaccination, additional types of hybrid immunity may be of interest to evaluate, such as vaccination followed by infection. A more thorough assessment of cytokine-independent functions expressed by SARS-CoV-2–specific T cells is required to understand their role in mediating hybrid immunity, as well as vaccine- and infection-induced immunity more generally.

Acknowledgments

We acknowledge Teresa K. Rodriguez for technical assistance with flow cytometry and Malisa T. Smith and Emma Bishop for assistance with data analysis. Staff at BioLegend assisted with upstream data processing. Seattle Genomics service core of the Washington National Primate Research Center assisted with 10× library preparation and sequencing. Leanne Whitmore and Elise Smith assisted with read mapping, trimming, and quality control.

Disclosures

H.Y.C. reported consulting with Ellume, Pfizer, The Bill and Melinda Gates Foundation, GlaxoSmithKline, Janssen, and Merck. H.Y.C. has received research funding from Gates Ventures and Sanofi Pasteur, and support and reagents from Ellume and Cepheid outside of the submitted work. The other authors have no financial conflicts of interest.

References

1. Abu-Raddad, L. J., H. Chemaitelly, H. H. Ayoub, H. M. Yassine, F. M. Benslimane, H. A. Al Khatib, P. Tang, M. R. Hasan, P. Coyle, Z. Al Kanaani, et al. 2021. Association of prior SARS-CoV-2 infection with risk of breakthrough infection following mRNA vaccination in Qatar. *JAMA* 326: 1930–1939.
2. Plotkin, S. A., and P. B. Gilbert. 2012. Nomenclature for immune correlates of protection after vaccination. *Clin. Infect. Dis.* 54: 1615–1617.
3. Gilbert, P. B., D. C. Montefiori, A. B. McDermott, Y. Fong, D. Benkeser, W. Deng, H. Zhou, C. R. Houchens, K. Martins, L. Jayashankar, et al.; Immune Assays Team; Moderna, Inc. Team; Coronavirus Vaccine Prevention Network (CoVPN)/Coronavirus Efficacy (COVE) Team; United States Government (USG)/CoVPN Biostatistics Team. 2022. Immune correlates analysis of the mRNA-1273 COVID-19 vaccine efficacy clinical trial. *Science* 375: 43–50.
4. Planas, D., D. Veyer, A. Baidaliuk, I. Staropoli, F. Guivel-Benhassine, M. M. Rajah, C. Planchais, F. Porrot, N. Robillard, J. Puech, et al. 2021. Reduced sensitivity of SARS-CoV-2 variant Delta to antibody neutralization. *Nature* 596: 276–280.
5. Planas, D., N. Saunders, P. Maes, F. Guivel-Benhassine, C. Planchais, J. Buchrieser, W. H. Bolland, F. Porrot, I. Staropoli, F. Lemoine, et al. 2022. Considerable escape of SARS-CoV-2 Omicron to antibody neutralization. *Nature* 602: 671–675.
6. Tarke, A., J. Sidney, N. Methot, E. D. Yu, Y. Zhang, J. M. Dan, B. Goodwin, P. Rubiro, A. Sutherland, E. Wang, et al. 2021. Impact of SARS-CoV-2 variants on the total $CD4^+$ and $CD8^+$ T cell reactivity in infected or vaccinated individuals. *Cell Rep. Med.* 2: 100355.
7. Keeton, R., M. B. Tincho, A. Ngomti, R. Baguma, N. Benede, A. Suzuki, K. Khan, S. Cele, M. Bernstein, F. Karim, et al. 2022. T cell responses to SARS-CoV-2 spike cross-recognize Omicron. [Published erratum appears in 2022 *Nature* 604: e25.] *Nature* 603: 488–492.
8. Rodda, L. B., P. A. Morawski, K. B. Pruner, M. L. Fahning, C. A. Howard, N. Franko, J. Logue, J. Eggenberger, C. Stokes, I. Golez, et al. 2022. Imprinted SARS-CoV-2-specific memory lymphocytes define hybrid immunity. *Cell* 185: 1588–1601.e14.
9. Minervina, A. A., M. V. Pogorelyy, A. M. Kirk, J. C. Crawford, E. K. Allen, C. H. Chou, R. C. Mettelman, K. J. Allison, C. Y. Lin, D. C. Brice, et al.; SJTRC Study Team. 2022. SARS-CoV-2 antigen exposure history shapes phenotypes and specificity of memory $CD8^+$ T cells. *Nat. Immunol.* 23: 781–790.
10. Chu, H. Y., J. A. Englund, L. M. Starita, M. Famulare, E. Brandstetter, D. A. Nickerson, M. J. Rieder, A. Adler, K. Lacombe, A. E. Kim, et al.; Seattle Flu Study Investigators. 2020. Early detection of Covid-19 through a citywide pandemic surveillance platform. *N. Engl. J. Med.* 383: 185–187.
11. Harris, P. A., R. Taylor, R. Thielke, J. Payne, N. Gonzalez, and J. G. Conde. 2009. Research electronic data capture (REDCap)—a metadata-driven methodology and workflow process for providing translational research informatics support. *J. Biomed. Inform.* 42: 377–381.
12. Yu, K. K., S. Fischinger, M. T. Smith, C. Atyeo, D. Cizmeci, C. R. Wolf, E. D. Layton, J. K. Logue, M. S. Aguilar, K. Shuey, et al. 2021. Comorbid illnesses are associated with altered adaptive immune responses to SARS-CoV-2. *JCI Insight* 6: e146242.
13. Stillwell, R., and B. E. Bierer. 2001. T cell signal transduction and the role of CD7 in costimulation. *Immunol. Res.* 24: 31–52.
14. Hao, Y., S. Hao, E. Andersen-Nissen, W. M. Mauck III, S. Zheng, A. Butler, M. J. Lee, A. J. Wilk, C. Darby, M. Zager, et al. 2021. Integrated analysis of multimodal single-cell data. *Cell* 184: 3573–3587.e29.
15. McGinnis, C. S., D. M. Patterson, J. Winkler, D. N. Conrad, M. Y. Hein, V. Srivastava, J. L. Hu, L. M. Murrow, J. S. Weissman, Z. Werb, et al. 2019. MULTI-seq: sample multiplexing for single-cell RNA sequencing using lipid-tagged indices. *Nat. Methods* 16: 619–626.
16. Borcherding, N., N. L. Bormann, and G. Kraus. 2020. scRepertoire: an R-based toolkit for single-cell immune receptor analysis. *F1000 Res.* 9: 47.
17. Wickham, H. 2016. ggplot2: elegant graphics for data analysis. In: *Use R!* 2nd Ed. Springer-Verlag, New York, p. 1–260.
18. Finak, G., J. Frelinger, W. Jiang, E. W. Newell, J. Ramey, M. M. Davis, S. A. Kalams, S. C. De Rosa, and R. Gottardo. 2014. OpenCyto: an open source infrastructure for scalable, robust, reproducible, and automated, end-to-end flow cytometry data analysis. *PLOS Comput. Biol.* 10: e1003806.
19. Lin, L., G. Finak, K. Ushey, C. Seshadri, T. R. Hawn, N. Frahm, T. J. Scriba, H. Mahomed, W. Hanekom, P. A. Bart, et al. 2015. COMPASS identifies T-cell subsets correlated with clinical outcomes. *Nat. Biotechnol.* 33: 610–616.
20. Gu, Z., R. Eils, and M. Schlesner. 2016. Complex heatmaps reveal patterns and correlations in multidimensional genomic data. *Bioinformatics* 32: 2847–2849.
21. Melville, J. 2021. uwot: The uniform manifold approximation and projection (UMAP) method for dimensionality reduction. https://CRAN.R-project.org/package=uwot.
22. Fonseka, C. Y., D. A. Rao, N. C. Teslovich, I. Korsunsky, S. K. Hannes, K. Slowikowski, M. F. Gurish, L. T. Donlin, J. A. Lederer, M. E. Weinblatt, et al. 2018. Mixed-effects association of single cells identifies an expanded effector $CD4^+$ T cell subset in rheumatoid arthritis. *Sci. Transl. Med.* 10: eaaq0305.
23. Bates, D., M. Mächler, B. Bolker, and S. Walker. 2015. Fitting linear mixed-effects models using lme4. *J. Stat. Softw.* 67: 1–48.
24. Jackson, L. A., E. J. Anderson, N. G. Rouphael, P. C. Roberts, M. Makhene, R. N. Coler, M. P. McCullough, J. D. Chappell, M. R. Denison, L. J. Stevens, et al.; mRNA-1273 Study Group. 2020. An mRNA vaccine against SARS-CoV-2—preliminary report. *N. Engl. J. Med.* 383: 1920–1931.
25. Sahin, U., A. Muik, I. Vogler, E. Derhovanessian, L. M. Kranz, M. Vormehr, J. Quandt, N. Bidmon, A. Ulges, A. Baum, et al. 2021. BNT162b2 vaccine induces neutralizing antibodies and poly-specific T cells in humans. *Nature* 595: 572–577.
26. Grifoni, A., D. Weiskopf, S. I. Ramirez, J. Mateus, J. M. Dan, C. R. Moderbacher, S. A. Rawlings, A. Sutherland, L. Premkumar, R. S. Jadi, et al. 2020. Targets of T cell responses to SARS-CoV-2 coronavirus in humans with COVID-19 disease and unexposed individuals. *Cell* 181: 1489–1501.e15.
27. Braun, J., L. Loyal, M. Frentsch, D. Wendisch, P. Georg, F. Kurth, S. Hippenstiel, M. Dingeldey, B. Kruse, F. Fauchere, et al. 2020. SARS-CoV-2-reactive T cells in healthy donors and patients with COVID-19. *Nature* 587: 270–274.
28. Mateus, J., A. Grifoni, A. Tarke, J. Sidney, S. I. Ramirez, J. M. Dan, Z. C. Burger, S. A. Rawlings, D. M. Smith, E. Phillips, et al. 2020. Selective and cross-reactive SARS-CoV-2 T cell epitopes in unexposed humans. *Science* 370: 89–94.
29. Oberhardt, V., H. Luxenburger, J. Kemming, I. Schulien, K. Ciminski, S. Giese, B. Csernalabics, J. Lang-Meli, I. Janowska, J. Staniek, et al. 2021. Rapid and stable mobilization of $CD8^+$ T cells by SARS-CoV-2 mRNA vaccine. *Nature* 597: 268–273.
30. Sekine, T., A. Perez-Potti, O. Rivera-Ballesteros, K. Strålin, J.-B. Gorin, A. Olsson, S. Llewellyn-Lacey, H. Kamal, G. Bogdanovic, S. Muschiol; Karolinska COVID-19 Study Group; et al. 2020. Robust T cell immunity in convalescent individuals with asymptomatic or mild COVID-19. *Cell* 183: 158–168.e14.
31. Hewitson, J. P., K. A. West, K. R. James, G. F. Rani, N. Dey, A. Romano, N. Brown, S. A. Teichmann, P. M. Kaye, and D. Lagos. 2020. *Malat1* suppresses immunity to infection through promoting expression of Maf and IL-10 in Th cells. *J. Immunol.* 204: 2949–2960.
32. Nish, S. A., K. D. Zens, R. Kratchmarov, W. W. Lin, W. C. Adams, Y. H. Chen, B. Yen, N. J. Rothman, A. Bhandoola, H. H. Xue, et al. 2017. CD4+ T cell effector commitment coupled to self-renewal by asymmetric cell divisions. *J. Exp. Med.* 214: 39–47.
33. Sharma, P. K., E. B. Wong, R. J. Napier, W. R. Bishai, T. Ndung'u, V. O. Kasprowicz, D. A. Lewinsohn, D. M. Lewinsohn, and M. C. Gold. 2015. High expression of CD26 accurately identifies human bacteria-reactive MR1-restricted MAIT cells. *Immunology* 145: 443–453.
34. Ng, S. S., F. De Labastida Rivera, J. Yan, D. Corvino, I. Das, P. Zhang, R. Kuns, S. B. Chauhan, J. Hou, X. Y. Li, et al. 2020. The NK cell granule protein NKG7 regulates cytotoxic granule exocytosis and inflammation. *Nat. Immunol.* 21: 1205–1218.
35. Lin, Y., T. J. Roberts, V. Sriram, S. Cho, and R. R. Brutkiewicz. 2003. Myeloid marker expression on antiviral CD8+ T cells following an acute virus infection. *Eur. J. Immunol.* 33: 2736–2743.
36. Diamond, M. S., and M. Farzan. 2013. The broad-spectrum antiviral functions of IFIT and IFITM proteins. *Nat. Rev. Immunol.* 13: 46–57.
37. Cano-Gamez, E., B. Soskic, T. I. Roumeliotis, E. So, D. J. Smyth, M. Baldrighi, D. Willé, N. Nakic, J. Esparza-Gordillo, C. G. C. Larminie, et al. 2020. Single-cell transcriptomics identifies an effectorness gradient shaping the response of $CD4^+$ T cells to cytokines. *Nat. Commun.* 11: 1801.
38. Anderson, E. J., N. G. Rouphael, A. T. Widge, L. A. Jackson, P. C. Roberts, M. Makhene, J. D. Chappell, M. R. Denison, L. J. Stevens, A. J. Pruijssers, et al.; mRNA-1273 Study Group. 2020. Safety and immunogenicity of SARS-CoV-2 mRNA-1273 vaccine in older adults. *N. Engl. J. Med.* 383: 2427–2438.
39. Walsh, E. E., R. W. Frenck, Jr., A. R. Falsey, N. Kitchin, J. Absalon, A. Gurtman, S. Lockhart, K. Neuzil, M. J. Mulligan, R. Bailey, et al. 2020. Safety and immunogenicity of two RNA-based Covid-19 vaccine candidates. *N. Engl. J. Med.* 383: 2439–2450.
40. Sahin, U., A. Muik, I. Vogler, E. Derhovanessian, L. M. Kranz, M. Vormehr, J. Quandt, N. Bidmon, A. Ulges, A. Baum, et al. 2021. BNT162b2 vaccine induces neutralizing antibodies and poly-specific T cells in humans. *Nature* 595: 572–577.

Downloaded from http://aai.silverchair.com/jimmunol/article-pdf/210/9/1236/1645127/ji2200815.pdf by guest on 09 April 2024

41. Polack, F. P., S. J. Thomas, N. Kitchin, J. Absalon, A. Gurtman, S. Lockhart, J. L. Perez, G. Pérez Marc, E. D. Moreira, C. Zerbini, et al.; C4591001 Clinical Trial Group. 2020. Safety and efficacy of the BNT162b2 mRNA Covid-19 vaccine. *N. Engl. J. Med.* 383: 2603–2615.
42. Mateus, J., J. M. Dan, Z. Zhang, C. Rydyznski Moderbacher, M. Lammers, B. Goodwin, A. Sette, S. Crotty, and D. Weiskopf. 2021. Low-dose mRNA-1273 COVID-19 vaccine generates durable memory enhanced by cross-reactive T cells. *Science* 374: eabj9853.
43. McMahan, K., J. Yu, N. B. Mercado, C. Loos, L. H. Tostanoski, A. Chandrashekar, J. Liu, L. Peter, C. Atyeo, A. Zhu, et al. 2021. Correlates of protection against SARS-CoV-2 in rhesus macaques. *Nature* 590: 630–634.
44. Singh, D. K., E. Aladyeva, S. Das, B. Singh, E. Esaulova, A. Swain, M. Ahmed, J. Cole, C. Moodley, S. Mehra, et al. 2022. Myeloid cell interferon responses correlate with clearance of SARS-CoV-2. *Nat. Commun.* 13: 679.
45. Chilunda, V., P. Martinez-Aguado, L. C. Xia, L. Cheney, A. Murphy, V. Veksler, V. Ruiz, T. M. Calderon, and J. W. Berman. 2021. Transcriptional changes in CD16+ monocytes may contribute to the pathogenesis of COVID-19. *Front. Immunol.* 12: 665773.
46. Ssemaganda, A., H. M. Nguyen, F. Nuhu, N. Jahan, C. M. Card, S. Kiazyk, G. Severini, Y. Keynan, R. C. Su, H. Ji, et al. 2022. Expansion of cytotoxic tissue-resident $CD8^+$ T cells and $CCR6^+CD161^+$ $CD4^+$ T cells in the nasal mucosa following mRNA COVID-19 vaccination. *Nat. Commun.* 13: 3357.
47. Monteiro, P., A. Gosselin, V. S. Wacleche, M. El-Far, E. A. Said, H. Kared, N. Grandvaux, M. R. Boulassel, J. P. Routy, and P. Ancuta. 2011. Memory CCR6+CD4+ T cells are preferential targets for productive HIV type 1 infection regardless of their expression of integrin β7. *J. Immunol.* 186: 4618–4630.
48. Altarawneh, H. N., H. Chemaitelly, H. H. Ayoub, P. Tang, M. R. Hasan, H. M. Yassine, H. A. Al-Khatib, M. K. Smatti, P. Coyle, Z. Al-Kanaani, et al. 2022. Effects of previous infection and vaccination on symptomatic Omicron infections. *N. Engl. J. Med.* 387: 21–34.
49. Centers for Disease Control and Prevention. 2022. Interim clinical considerations for use of COVID-19 vaccines: appendices, references, and previous updates. Atlanta, GA: Centers for Disease Control and Prevention. Available at: https://www.cdc.gov/vaccines/covid-19/clinical-considerations/interim-considerations-us-appendix.html.
50. Maringer, Y., A. Nelde, S. M. Schroeder, J. Schuhmacher, S. Hörber, A. Peter, J. Karbach, E. Jäger, and J. S. Walz. 2022. Durable spike-specific T cell responses after different COVID-19 vaccination regimens are not further enhanced by booster vaccination. *Sci. Immunol.* 7: eadd3899.
51. Schmidt, T., V. Klemis, D. Schub, J. Mihm, F. Hielscher, S. Marx, A. Abu-Omar, L. Ziegler, C. Guckelmus, R. Urschel, et al. 2021. Immunogenicity and reactogenicity of heterologous ChAdOx1 nCoV-19/mRNA vaccination. *Nat. Med.* 27: 1530–1535.
52. Hillus, D., T. Schwarz, P. Tober-Lau, K. Vanshylla, H. Hastor, C. Thibeault, S. Jentzsch, E. T. Helbig, L. J. Lippert, P. Tscheak, et al.; EICOV/COVIM Study Group. 2021. Safety, reactogenicity, and immunogenicity of homologous and heterologous prime-boost immunisation with ChAdOx1 nCoV-19 and BNT162b2: a prospective cohort study. *Lancet Respir. Med.* 9: 1255–1265.

Downloaded from http://aai.silverchair.com/jimmunol/article-pdf/210/9/1236/1645127/ji2200815.pdf by guest on 09 April 2024